

Quasiparticle-continuum level repulsion in a quantum magnet

K.W. Plumb,¹ Kyusung Hwang,¹ Y. Qiu,^{2,3} Leland W. Harriger,²
 G. E. Granroth,⁴ Alexander I. Kolesnikov,⁵ G. J. Shu,⁶ F.C.
 Chou,⁶ Ch. Rüegg,^{7,8} Yong Baek Kim,^{1,9} and Young-June Kim¹

¹*Department of Physics and Center for Quantum Materials,
 University of Toronto, Toronto, Ontario M5S 1A7, Canada*

²*NIST Center for Neutron Research,
 National Institute of Standards and Technology,
 Gaithersburg, Maryland 20899, USA*

³*Department of Materials Science and Engineering,
 University of Maryland, College Park, Maryland 20742, USA*

⁴*Neutron Data Analysis and Visualization Division,
 Oak Ridge National Laboratory, Oak Ridge, Tennessee 37831, USA*

⁵*Spallation Neutron Source, Oak Ridge National Laboratory,
 Oak Ridge, Tennessee 37831, USA*

⁶*Center for Condensed Matter Sciences,
 National Taiwan University, Taipei, 10617 Taiwan*

⁷*Laboratory for Neutron Scattering and Imaging,
 Paul Scherrer Institute, CH-5232 Villigen, Switzerland*

⁸*Department of Quantum Matter Physics,
 University of Geneva, CH-1211 Geneva, Switzerland*

⁹*Canadian Institute for Advanced Research/Quantum Materials Program,
 Toronto, Ontario MSG 1Z8, Canada*

When the energy eigenvalues of two coupled quantum states approach each other in a certain parameter space, their energy levels repel each other and level crossing is avoided. Such level repulsion, or avoided level crossing, is commonly used to describe the dispersion relation of quasiparticles in solids. However, little is known about the level repulsion when more than two quasiparticles are present; for example, in an open quantum system where a quasiparticle can spontaneously decay into many particle continuum. Here we show that even in this case level repulsion exists between a long-lived quasiparticle state and a continuum. In our fine resolution neutron spectroscopy study of magnetic quasiparticles in a frustrated quantum magnet BiCu_2PO_6 , we observe a renormalization of quasiparticle dispersion relation due to the presence of the continuum of multi-quasiparticle states. Our results have a broad implication for understanding open quantum systems described by non-hermitian Hamiltonian.

A fundamental concept in condensed matter physics is the idea that strongly interacting atomic systems can be treated as a collection of weakly interacting and long-lived quasiparticles. Within a quasiparticle picture, complex collective excited states in a many body system are described in terms of effective elementary excitations. The quanta of these excitations carry a definite momentum and energy and are termed quasiparticles. Magnetic insulators containing localized $S = 1/2$ magnetic moments and having valence bond solid ground states are ideal systems in which to study bosonic quasiparticles in an interacting quantum many body system [1]. The elementary magnetic excitations in these materials are triply-degenerate $S = 1$ quasiparticles called triplons, and their momentum and energy resolved dynamics can be probed directly through inelastic neutron scattering.

In particular, when the system's Hamiltonian has an interaction term coupling single and multi-particle states, the single quasiparticles may decay into the continuum of multiparticle states [2, 3]. Therefore, an ensemble of quasiparticles as may be realized in a quantum magnet is a good example of an open quantum system, in which particle number is not conserved. [4] In such a system, the energy eigenvalues are in general complex, and the particles have a finite lifetime, which is given by the imaginary part of the complex eigenvalue [5]. It was shown that even in the case of an open quantum system, the avoided level crossing could occur in the complex plane [6].

Despite broad interest in interacting open quantum systems, experimentally realizing

an ideal condition to study the interaction between a quasiparticle and a multi-particle continuum turns out to be extremely difficult. Here we show that the quantum magnet BiCu_2PO_6 presents a rare model system that allows one to study quasiparticle level repulsion in the complex plane. This phenomena arises due to the presence of the very large anisotropic exchange interactions in BiCu_2PO_6 , originating from spin-orbit coupling (SOC). These anisotropic interactions play a dual role in BiCu_2PO_6 . First, they break the degeneracy of the triplet excitations, making the triplon dispersion relation non-degenerate in phase space. In addition, the anisotropic exchange interaction is responsible for the strong anharmonicity which couples the single and multi-triplon excitations. As a result, the triplon lifetime may be reduced in the region of phase space where (single) triplon dispersion overlaps with multi-triplon continuum. This decay process may in fact be so strong that the quasiparticle description ceases to be valid within the continuum. Furthermore, we show that the dispersion relation of the triplons is strongly renormalized near the boundary of the multi-triplon continuum due to the level repulsion between the single quasiparticle and the continuum.

In the following, we first present inelastic neutron scattering (INS) measurements of the full triplon dispersion in BiCu_2PO_6 , which reveal a rich excitation spectrum including a multi-triplon continuum of scattering. Analysis of the triplon excitation spectrum using bond-operator theory enables us to determine the magnetic Hamiltonian of BiCu_2PO_6 accurately. We find that strong spin-orbit coupling plays an essential role in this compound through substantial symmetric and antisymmetric anisotropic interactions. We will finally discuss the interaction of the triplon quasiparticles with the continuum which manifests as a drastic renormalization of the quasiparticle spectra and ultimately spontaneous quasiparticle decay.

VALENCE BOND SOLID

The orthorhombic crystal structure of BiCu_2PO_6 is shown in Fig. 1 (a); the structure contains zig-zag chains of Cu^{2+} ions running parallel to the b-axis. Magnetic interactions along the chains are frustrated because of a competition between the nearest-neighbor (NN) and next-nearest-neighbor (NNN) antiferromagnetic exchange terms J_1 and J_2 . The frustrated chains are coupled strongly along the c-axis by antiferromagnetic coupling J_4 to form

a two-leg ladder. As a result of the strong antiferromagnetic coupling J_4 , two spins on each rung can form singlets, and the ground state is described as an array of singlets termed a valence bond solid. The elementary excitations in this case are triplets that can propagate along the chain direction due to J_1 and J_2 . Within a single (ladder) bilayer, there are two crystallographically inequivalent copper sites (Cu_A and Cu_B as shown in Fig. 1 (a)). This results in the breaking of inversion symmetry across all magnetic bonds, and consequently anisotropic interactions are permitted in the magnetic Hamiltonian, as will be discussed later.

The dispersion relation, which contains essential information regarding the triplon dynamics such as the effective mass and velocity, is revealed directly by inelastic neutron scattering. Before discussing our neutron scattering measurements, it is helpful to briefly review the expected excitation spectrum of the frustrated two-leg ladder as realized by BiCu_2PO_6 , first ignoring any anisotropic interactions. In the strong coupling limit of $J_1, J_2 \ll J_4$, the expected excitation spectrum is schematically illustrated in the inset of Fig. 1 (b)[8, 9]. The dispersion has a distinct W shape with minimum at an incommensurate wavevector. The incommensurate minimum of the gapped spectrum is the manifestation of the magnetic frustration in BiCu_2PO_6 ; since BiCu_2PO_6 contains two singlet dimers per unit cell, there are two separate bands of triplons. The bands become degenerate at the point $k = 0.5$ and are related by a simple folding of the zone with the minima of each band appearing at incommensurate wavevectors $k = 0.5 \pm \delta$. Anisotropic interactions entering the magnetic Hamiltonian may then further split the degeneracy of each triplon band.

An overview of the zero field INS measurements is presented in Fig. 1 (b). The gapped, W-shaped, dispersion of each branch is clearly visible at both $h=0$ and 3 with a bandwidth of 25 meV, and incommensurate minima at $k = 0.575$ and $k = 0.425$ in (a) and (b) respectively. We have not observed any dispersion along the \mathbf{h} -direction confirming the weak inter-bilayer coupling; however, intensities are strongly modulated with momentum transfers along h . This effect is most clearly shown in Fig. 1 (d) where the intensity along the two dimensional rods of scattering, at $k = 0.5 \pm 0.075$ positions, is plotted. The modulation arises from the bilayer structure factor: interference between the scattering from the two layers within a bilayer. For weak inter-bilayer coupling the bilayer structure factor can be written simply in the following form $B^i(\mathbf{Q}) = A \cos\left(\frac{1}{2}\mathbf{Q} \cdot a'\hat{\mathbf{h}} + \phi^i\right)$, where a' is the intrabilayer spacing, shown in Fig. 1 (a), $\hat{\mathbf{h}}$ is a unit vector directed along \mathbf{h} , ϕ^i is a phase factor for the mode indexed by

i , and A is an arbitrary amplitude factor. Solid lines in Fig. 1 (d) are the bilayer structure factor with the known intrabilayer spacing for BiCu_2PO_6 of $a'=0.162a$, and $\phi^i=0$ and $\pi/2$ for the modes with minima at $k = 0.575$ and $k = 0.425$ respectively.

What makes BiCu_2PO_6 unique among valence bond solids is the presence of strong anisotropic interactions that qualitatively alter the nature of the triplons. The evidence for anisotropic interactions in BiCu_2PO_6 is first borne out by high resolution measurements around the incommensurate wavevector at $\mathbf{Q} = (0, 0.575, 1)$ shown in Fig. 1 (c). These reveal that anisotropies in BiCu_2PO_6 completely split the degeneracy of each primary branch such that three distinct modes are observed. Note that the intensity modulation of the primary modes by the bi-layer structure factor enables the independent probing of each mode. Anisotropy splitting is significant, with the minima of each mode corresponding to gap values of $\Delta_1=1.67(2)$ meV, $\Delta_2=2.85(5)$ meV, and $\Delta_3=3.90(5)$ meV.

The quantum states of each mode can be further explored via INS measurements performed with applied magnetic fields. The neutron intensities for applied fields of 4, 8, and 11 T are plotted in Fig. 2. No further splitting of the modes was observed indicating that anisotropic interactions in the Hamiltonian have completely lifted the $\text{SU}(2)$ spin rotation symmetry [10]. Constant momentum-transfer cuts around the incommensurate wavevector, Fig. 2 (d)-(f), reveal an anomalous Zeeman behaviour. Rather than splitting into the conventional ordering in energy of $S_z = \{+1, 0, -1\}$ [1, 11], the lowest energy mode exhibits negligible field dependence and is assigned a $S_z = 0$ quantum state, while the two higher energy modes have the Zeeman character of $S_z = +1$ and $S_z = -1$ respectively. (See the field dependence plotted in Fig. 3c.) [12]

NON-INTERACTING TRIPLONS

The complete dispersion extracted from INS measurements, combining the data for $h = 0$ and $h = 3$, is plotted in Fig. 3. There are six triplon modes, two bands arise from two inequivalent dimers per unit cell which are each further split into three non-degenerate modes by anisotropic interactions.

To understand the spin dynamics in BiCu_2PO_6 we consider a generic spin Hamiltonian

with Heisenberg J_{ij} , as well as antisymmetric \mathbf{D}_{ij} and symmetric anisotropic $\Gamma_{ij}^{\mu\nu}$ interactions

$$\begin{aligned}\mathcal{H} = & \sum_{i>j} (J_{ij} \mathbf{S}_i \cdot \mathbf{S}_j + \mathbf{D}_{ij} \cdot \mathbf{S}_i \times \mathbf{S}_j + \Gamma_{ij}^{\mu\nu} S_i^\mu S_j^\nu) \\ & - g\mu_B \mathbf{H} \cdot \sum_i \mathbf{S}_i,\end{aligned}\quad (1)$$

in which the symmetric anisotropy term is constrained by the relation

$$\Gamma_{ij}^{\mu\nu} = \frac{D_{ij}^\mu D_{ij}^\nu}{2J_{ij}} - \frac{\delta^{\mu\nu} \mathbf{D}_{ij}^2}{4J_{ij}}. \quad (2)$$

Both the antisymmetric Dzyaloshinskii-Moriya (DM) and symmetric (Γ) anisotropic exchange terms originate from spin-orbit coupling [13–16]. While the symmetric anisotropy term is the smaller of the two, and is often neglected, it can have pronounced effects on the magnetic ground state and excitation spectrum [17]. Employing a quadratic (non-interacting) bond operator theory (BOT) [1–3], for the valence-bond ordered ground state with valence bonds on J_4 links, we have found that the INS data is best described with the following coupling constants: $J_1 = J_2 = J_4 = 8$ meV, $J_3 = 1.6$ meV, $D_1^a = 0.6J_1$, $D_1^b = 0.45J_1$, $\Gamma_1^{aa} = 0.039J_1$, $\Gamma_1^{bb} = -0.039J_1$, and $\Gamma_1^{ab} = \Gamma_1^{ba} = 0.135J_1$ [21]; the calculated triplon dispersion is plotted in Fig. 3 (a) and (b). At quadratic order, the BOT captures important details of the low energy spectra including the slight shift of incommensurate minima between each branch, as well as the overall bandwidth of the excitations. Importantly, this calculation appropriately describes the anomalous Zeeman splitting plotted in Fig. 3 (c). Furthermore, extending the BOT [22] to determine the field dependence of each mode for fields applied along the **b** and **c** directions correctly predicts the hierarchy of critical fields measured previously $H_c^a > H_c^b > H_c^c$. [4] The quadratic BOT is essentially a mean-field expansion and so is likely to overestimate the coupling constants. However, even within the mean field estimation, it is remarkable that such large anisotropic interactions are required to describe magnetic excitations in BiCu2PO6.

While the BOT describes the overall features of the measured triplon dispersion, this quadratic theory fails to capture some very distinct features of the spectrum, including a bending of the triplon modes around $k_c \approx 1 \pm 0.26$ in Fig. 3 (a). Here the single triplon dispersions are strongly renormalized, bending away from the quadratic dispersion, in an avoided crossing with a multi-triplon continuum. In addition, the dispersion abruptly stops beyond the critical wavevector of $k_c \approx 0.75$. As we will discuss below, these dynamics

ultimately arise as a consequence of the anharmonic magnetic interactions which couple single triplon quasiparticles with multi-triplon continuum states.

MULTIPARTICLE CONTINUUM AND LEVEL REPULSION

The presence of large anisotropic exchange interactions has dramatic implications on the behaviour of triplons in this system. In contrast to isotropic quantum magnets where the triplon dynamics are typically well described in a harmonic expansion, the anisotropic exchange interactions in BiCu_2PO_6 produce significant anharmonic (cubic order in bond operators) couplings appearing as non-particle conserving terms in the bond-operator Hamiltonian. This anharmonicity modifies the triplon dispersion relation in BiCu_2PO_6 qualitatively. In figure 4 (b) the quantity $\hbar\omega S(\mathbf{Q}, \omega)$ is represented in the false color map. $\hbar\omega S(\mathbf{Q}, \omega)$ highlights the effects of multi-triplon interactions, including an avoided crossing and extinction of the lowest bands around $k = 0.8$ and a continuum of scattering at high energies around $k = 1$.

In addition to exciting a single-triplon quasiparticle, a neutron can create two or more triplon excitations simultaneously. For example, a neutron with momentum \mathbf{Q} can create two triplons with momentum \mathbf{q} and $\mathbf{Q} - \mathbf{q}$. These two-triplon excitations form a continuum with a lower bound determined by conservation of momentum and energy $\omega_{2t}(\mathbf{Q}) = \min_{\mathbf{q}} \{ \omega(\mathbf{q}) + \omega(\mathbf{Q} - \mathbf{q}) \}$, where $\omega(\mathbf{q})$ is the single-triplon dispersion. This lower boundary for two-triplon scattering, as determined from the quadratic dispersion, approximately delineates the region of continuum scattering shown in Fig. 4 (b). It is within this kinematic bound that the qualitative effects of anharmonic interactions in BiCu_2PO_6 are most apparent. Here the non-particle conserving terms offer decay channels for single triplon excitations. A physical consequence of this is that the triplon lifetime is significantly reduced, even in the absence of any thermal fluctuations. The effect manifests in a neutron scattering experiment as a strong damping of the quasiparticle peak. In Figs. 4 (c) and (d) the momentum dependent intensity and linewidth of each mode around $k = 0.8$ are shown, highlighting the different behaviour of each mode in this region. While we observe a continuous increase in the damping of the highest energy mode as it smoothly merges into the continuum, a much more dramatic effect is apparent in the two low energy triplon branches. The single triplon dispersions for these branches are strongly renormalized by interactions with the continuum, bending away from

the quadratic dispersion, in an avoided crossing as shown in Fig. 3 (a). In addition, these branches remain resolution limited in energy over all wave vectors, but terminate abruptly upon entering the continuum. This is a spectacular example of a spontaneous quasiparticle breakdown, where the decay channels are so effective that an appropriate description of the system in terms of quasiparticles does not exist [3, 24].

While detailed observations of triplon dynamics have been made in the past [25–27], clear examples of the spontaneous breakdown of a triplon spectrum as observed here are rare. In the two-dimensional correlated singlet material piperazinium hexachlorodicuprate (PHCC), a well defined triplon peak in the excitation spectrum was observed to abruptly merge with a continuum and vanish beyond a threshold momentum [2]. Somewhat different phenomena were observed in the organometallic two-leg ladder compound IPA-CuCl₃, in which the single triplon dispersion abruptly terminated beyond a critical wavevector, without damping nor two triplon continuum [28]. The decay process we observe in BiCu₂PO₆ is unique, as each triplon branch exhibits different decay behavior, as illustrated schematically in Fig. 4a. The highest energy mode does not bend, but merges smoothly with and decays into the continuum, in contrast to the behavior of the two lower energy branches. Since each single particle mode is associated with a different effective spin quantum number, this behaviour may be associated with branch dependent selection rules in the decay processes. Such an explicit manifestation of spin dependent quasiparticle interactions has not been observed before.

We would like to emphasize that the underlying magnetic interactions in BiCu₂PO₆ satisfies two crucial conditions for realizing strong coupling between the single and multiparticle states. First, the large bandwidth of triplon excitations relative to the gap energy at the incommensurate minima results in a large overlap between the single-triplon and continuum states. This overlap ensures that the kinematic conditions for the decay of a single-triplon are satisfied over a large region of phase space. Second, strong anharmonic interactions provide channels for coupling single and multi triplon states [3, 24]. The existence of magnetic interactions which couple single and multi-particle states are not always guaranteed. In BiCu₂PO₆, the Heisenberg exchange terms, J_1 , J_2 , and J_4 cancel at cubic order in an interacting bond operator theory and do not contribute to the spontaneous decay. It is the DM interactions which appear as the strongest anharmonic terms and, thus, are responsible for the spontaneous decay of single particle states into multiparticle ones.[29]

In summary, we have mapped the quasiparticle excitation spectra in the quantum magnet BiCu_2PO_6 through comprehensive INS measurements. The low energy triplon excitations are captured by a quadratic bond operator theory for the valence bond solid and we find that very large anisotropic interactions are necessary to describe the excitation spectrum. These anisotropic couplings appear as anharmonic, non particle conserving, terms in the bond operator Hamiltonian and manifest in a complete termination of the quasiparticle spectra beyond a critical wavevector. Strong hybridization between the lowest triplon branches and higher order continuum scattering in the neighbourhood of the critical wavevector results in a renormalization and avoided crossing in this open quantum system. Perhaps the most important feature of the excitation spectrum in BiCu_2PO_6 is this selective hybridization, renormalization, and termination of the two lowest branches, distinct from the smooth merging of the highest energy branch into a continuum. Further theoretical investigation of interacting triplons could shed light on the origin of the observed unusual decay behaviour.

Acknowledgments: We would also like to thank Götz Uhrig, Oleg Tchernyshyov and Se Kwon Kim for helpful discussions. This research was supported by NSERC of Canada, Canada Foundation for innovation, Canada Research Chairs program, and Centre for Quantum materials at the University of Toronto. Work at ORNL was sponsored by the Division of Scientific User Facilities, Office of Basic Energy Science, US department of Energy (DOE). Work at NIST utilized facilities supported in part by the National Science Foundation under Agreement No. DMR-0944772.

Methods: All measurements used the same 4.5 g single crystal as previous studies [30]. Magnetic excitations in BiCu_2PO_6 were mapped through INS measurements performed on a number of instruments. High energy time of flight neutron scattering measurements were carried out on the SEQUOIA spectrometer at the Spallation Neutron source covering the full dynamic range of excitations in BiCu_2PO_6 with high energy resolution $\Delta E \sim 0.8$ meV at the elastic line. Measurements on SEQUOIA were performed with a fixed incident neutron energy of $E_i = 40$ meV and the fine resolution Fermi-chopper (FC₂)[31] rotating at 360 Hz. The sample was mounted with the (h,k,0) plane lying in the horizontal scattering plane of the instrument and (h,0,0) initially aligned along the incident neutron wavevector \mathbf{k}_i . In order to map the complete dynamic structure factor $S(\mathbf{Q}, \omega)$ the sample was rotated through 180° in 0.5° steps. All measurements on SEQUOIA were performed with the sample held at a temperature of 4 K. Another set of high resolution measurements were conducted on the

SPINS cold triple axis spectrometer at the NIST center for neutron research. Here the sample was mounted in the $(0, k, l)$ scattering plane and all measurements used a fixed final energy of $E_f = 3.7$ meV employing a vertically focusing PG monochromator, a flat PG analyser, and a BeO filter between the sample and analyser. The spectrometer collimation sequence was Guide-80'-80'-Open resulting in an energy resolution of $\Delta E \sim 0.1$ meV at the elastic line. For the duration of the experiment, the sample was mounted on a Cu mount and temperature was controlled in a ^3He dilution refrigerator. Measurements in an applied magnetic field were carried out on the DCS time-of-flight spectrometer at NIST [32]. All measurements on DCS were performed using a fixed incident neutron wavelength of $\lambda_i = 2.9$ Å. The energy resolution on DCS was $\Delta E \sim 0.3$ meV at the elastic line. The sample was mounted in the $(0, k, l)$ scattering plane with $(0, 0, l)$ initially at 50° from the incident neutron beam and then rotated through 120° in 0.5° steps throughout the measurement. The sample was fixed on a Cu mount in a 11.5 T vertical field cryomagnet with a dilution refrigerators insert. A magnetic field between 4 and 11.5 T was applied along the a-axis and the sample was held at $T = 100$ mK for the duration of the measurements. Because of the very narrow magnet aperture, measurements on DCS were confined to the $(0, k, l)$ scattering plane with momentum transfers in the vertical direction limited to $h = 0 \pm 0.2$ r.l.u..

Author Contributions: K.W.P. and Y.-J.K. conceived the experiments. K.W.P., Y.Q., L.W.H. G.E.G, and A.I.K. performed the experiments and K.W.P. analysed the data. C.R. provided additional data. K.H. and Y.B.K. developed the theoretical model and performed calculations. G.J.S. and F.C.C. provided the sample. K.W.P. and Y.-J.K. wrote the paper with contributions from all co-authors.

- [1] T. Giamarchi, C. Rüegg, and O. Tchernyshyov, *Nat. Phys.* **4**, 198 (2008).
- [2] M. B. Stone, I. A. Zaliznyak, T. Hong, C. L. Broholm, and D. H. Reich, *Nature* **440**, 187 (2006).
- [3] M. E. Zhitomirsky and A. L. Chernyshev, *Rev. Mod. Phys.* **85**, 219 (2013).
- [4] The term, *open quantum system*, is often used in a different context, referring to a system that interacts with an environment, and follows stochastic dynamics. [See for example, H.-P. Breuer and F. Petruccione, *The theory of open quantum systems* (Oxford Univ. Press, Clarendon,

2007).] In this article, however, we are only concerned with a system described by non-hermitian Hamiltonian, in which particles can decay.

- [5] I. Rotter, *Journal of Physics A: Mathematical and Theoretical* **42**, 153001 (2009).
- [6] J. Okoowicz, M. Poszajczak, and I. Rotter, *Physics Reports* **374**, 271 (2003).
- [7] P. J. Brown, *International Tables for Crystallography*, Vol. C (Springer, Berlin, 2006) Chap. 4.4.5, pp. 454–461.
- [8] A. A. Tsirlin, I. Rousochatzakis, D. Kasinathan, O. Janson, R. Nath, F. Weickert, C. Geibel, A. M. Läuchli, and H. Rosner, *Phys. Rev. B* **82**, 144426 (2010).
- [9] A. Lavarélo, G. Roux, and N. Laflorencie, *Phys. Rev. B* **84**, 144407 (2011).
- [10] In this work, measurements in applied fields are all for the very narrow region $h=0\pm 0.2$ r.l.u. because the magnet aperture limited the detection of neutrons with momentum transfer out of the horizontal scattering plane.
- [11] M. Matsumoto, B. Normand, T. M. Rice, and M. Sigrist, *Phys. Rev. Lett.* **89**, 077203 (2002).
- [12] Of course, in the presence of anisotropic interactions the singlet and triplet wave functions are mixed and S_z is no longer a good quantum number. Here we assign each mode a pseudo S_z based on its Zeeman energy as this provides a convenient labelling scheme.
- [13] I. Dzyaloshinsky, *J. Phys. Chem. Solids* **4**, 241 (1958).
- [14] T. Moriya, *Phys. Rev.* **120**, 91 (1960).
- [15] L. Shekhtman, O. Entin-Wohlman, and A. Aharony, *Phys. Rev. Lett.* **69**, 836 (1992).
- [16] T. Yildirim, A. B. Harris, A. Aharony, and O. Entin-Wohlman, *Phys. Rev. B* **52**, 10239 (1995).
- [17] A. Zheludev, S. Maslov, I. Tsukada, I. Zaliznyak, L. P. Regnault, T. Masuda, K. Uchinokura, R. Erwin, and G. Shirane, *Phys. Rev. Lett.* **81**, 5410 (1998).
- [1] S. Sachdev and R. N. Bhatt, *Phys. Rev. B* **41**, 9323 (1990).
- [2] S. Gopalan, T. M. Rice, and M. Sigrist, *Phys. Rev. B* **49**, 8901 (1994).
- [3] M. Matsumoto, B. Normand, T. M. Rice, and M. Sigrist, *Phys. Rev. B* **69**, 054423 (2004).
- [21] See supplementary information for details of the bond operator theory.
- [22] See supplementary information for the calculated Zeeman behaviors of excitations for $H \parallel \mathbf{a}, \mathbf{b}, \mathbf{c}$.
- [4] Y. Kohama, S. Wang, A. Uchida, K. Prsa, S. Zvyagin, Y. Skourski, R. D. McDonald, L. Balicas, H. M. Rønnow, C. Rüegg, and M. Jaime, *Phys. Rev. Lett.* **109**, 167204 (2012).

- [24] M. E. Zhitomirsky, Phys. Rev. B **73**, 100404 (2006).
- [25] G. Xu, C. Broholm, D. H. Reich, and M. A. Adams, Phys. Rev. Lett. **84**, 4465 (2000).
- [26] M. B. Stone, I. Zaliznyak, D. H. Reich, and C. Broholm, Phys. Rev. B **64**, 144405 (2001).
- [27] S. Notbohm, P. Ribeiro, B. Lake, D. A. Tennant, K. P. Schmidt, G. S. Uhrig, C. Hess, R. Klingeler, G. Behr, B. Büchner, M. Reehuis, R. I. Bewley, C. D. Frost, P. Manuel, and R. S. Eccleston, Phys. Rev. Lett. **98**, 027403 (2007).
- [28] T. Masuda, A. Zheludev, H. Manaka, L. P. Regnault, J. H. Chung, and Y. Qiu, Phys. Rev. Lett. **96**, 047210 (2006).
- [29] A full theoretical treatment of triplon interactions is beyond the scope of this article, but such interactions will renormalize the DM parameters to somewhat smaller values. Nevertheless substantial D and Γ terms are essential for fitting the magnetic excitation spectra.
- [30] K. W. Plumb, Z. Yamani, M. Matsuda, G. J. Shu, B. Koteswararao, F. C. Chou, and Y.-J. Kim, Phys. Rev. B **88**, 024402 (2013).
- [31] G. E. Granroth, A. I. Kolesnikov, T. E. Sherline, J. P. Clancy, K. A. Ross, J. P. C. Ruff, B. D. Gaulin, and S. E. Nagler, Journal of Physics: Conference Series **251**, 012058 (2010).
- [32] J. Copley and J. Cook, Chemical Physics **292**, 477 (2003).

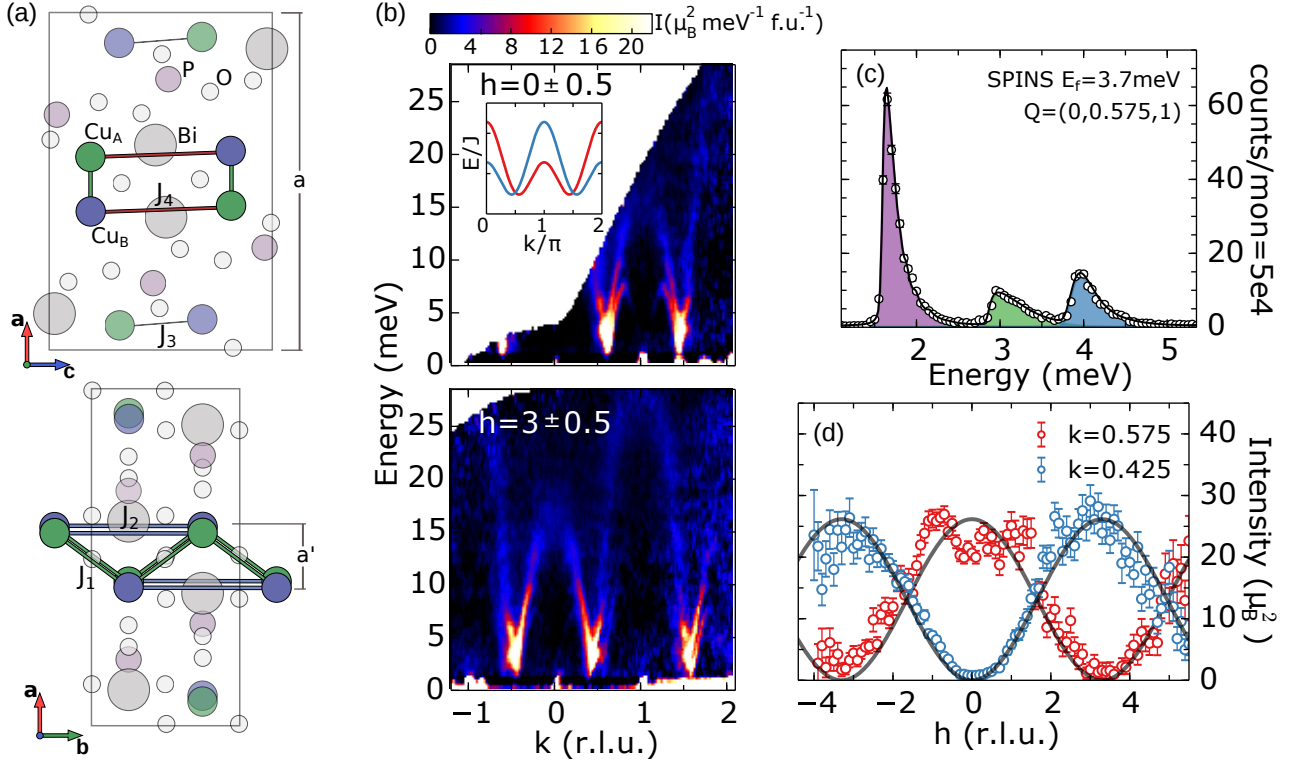


FIG. 1. (a) The orthorhombic crystal structure of BiCu_2PO_6 contains zig-zag chains of Cu^{2+} ions running parallel to the b -axis. The coupled chains can be viewed as bi-layers of Cu^{2+} with spacing $a' = 0.162a$. Along the chains neighboring Cu^{2+} interact via competing nearest-neighbor (NN) and next-nearest-neighbor (NNN) antiferromagnetic exchange terms J_1 and J_2 . The chains are coupled along the c -axis by J_4 to form a frustrated two-leg ladder, with an additional weak interladder exchange J_3 . (b) Energy-momentum slice of the inelastic neutron scattering intensity at $T = 4 \text{ K}$. Data have been corrected for the isotropic Cu^{2+} form-factor [7] and intensities placed into absolute units using the incoherent scattering from a vanadium standard. Inset is a schematic illustration of the dispersion of each mode. (c) Constant momentum transfer scan at the incommensurate wavevector $Q = (0, 0.575, 1)$ collected on the SPINS spectrometer at $T = 75 \text{ mK}$. Solid line is a fit to a resolution convolved model cross-section and filled areas are contributions from each mode. (d) Constant energy transfer cuts along two-dimensional rods of scattering at the $k = 0.5 \pm 0.075$ positions integrated over $E = 2 \pm 0.5 \text{ meV}$. Solid lines are the bilayer structure factor as described in the text. Error bars represent one standard deviation.

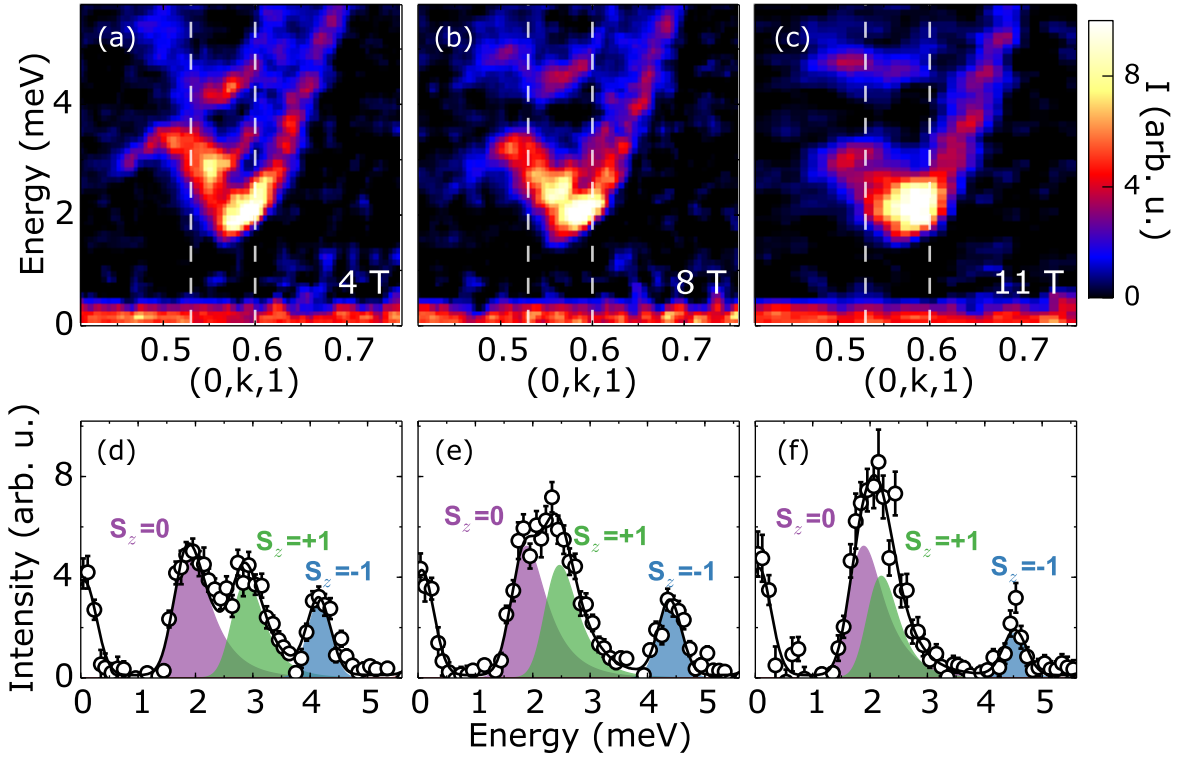


FIG. 2. Magnetic field dependence of dynamic magnetic correlations in BiCu_2PO_6 . (a)-(c) False color maps of the INS intensity measured on DCS at $T=100$ mK with magnetic field applied along the crystallographic **a**-axis. (d)-(f) Constant momentum transfer cuts integrated over $k = 0.565 \pm 0.035$ r.l.u. and $l = 1 \pm 0.05$ r.l.u., integration ranges are represented by dashed white lines in (a)-(c). Solid lines are fit to asymmetric Gaussian functions and filled areas show the contribution from each mode. Asymmetric line shapes result from the steep dispersion and extended momentum integration range. Error bars represent one standard deviation.

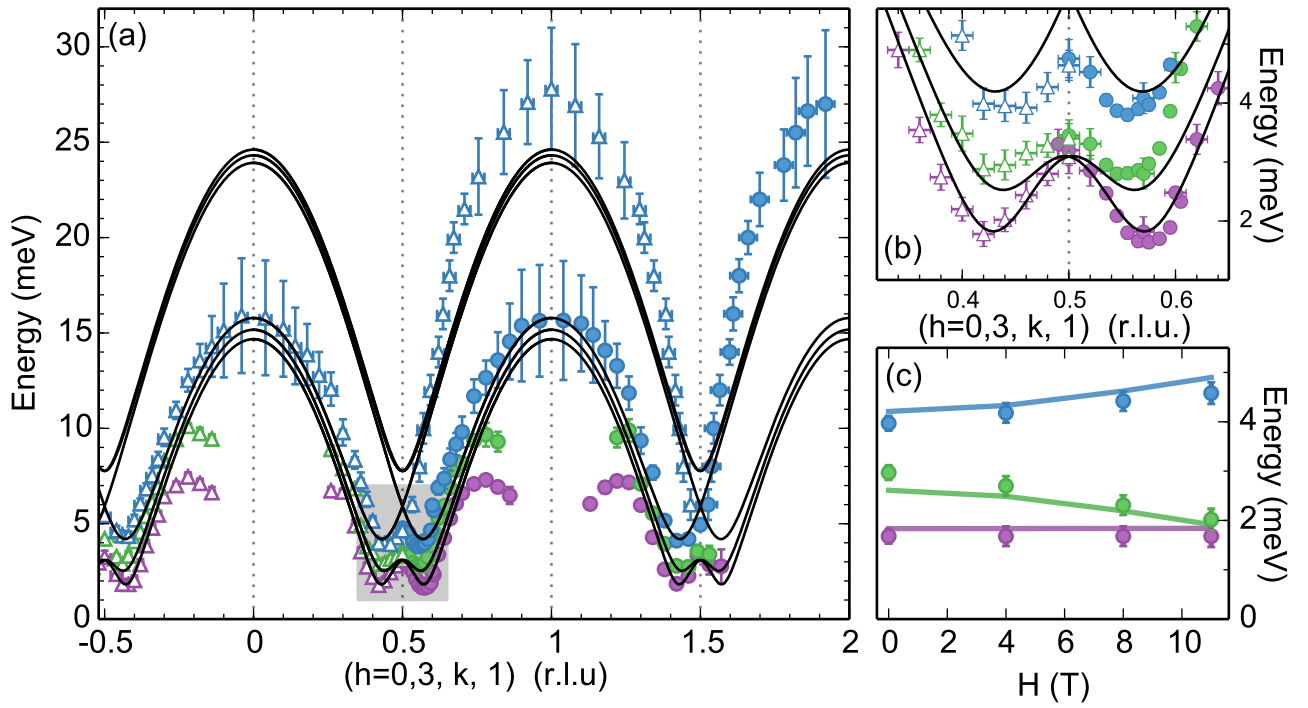


FIG. 3. (a) Dispersion of triplon excitations in BiCu_2PO_6 . Points extracted from fits to constant energy and momentum transfer scans from SEQUOIA and SPINS data sets. Filled circles correspond to $h = 0$, and open triangles correspond to $h = 3$. Solid lines are the dispersion calculated with a quadratic bond-operator theory as described in the text. (b) Detailed view around the point $k = 0.5 \pm 0.075$, indicated by the black shaded region in (a). (c) Measured energy of each mode at $Q = (0, 0.575, 1)$ as a function of applied magnetic field. Lines in (c) are the corresponding calculated Zeeman energies from the bond-operator theory.

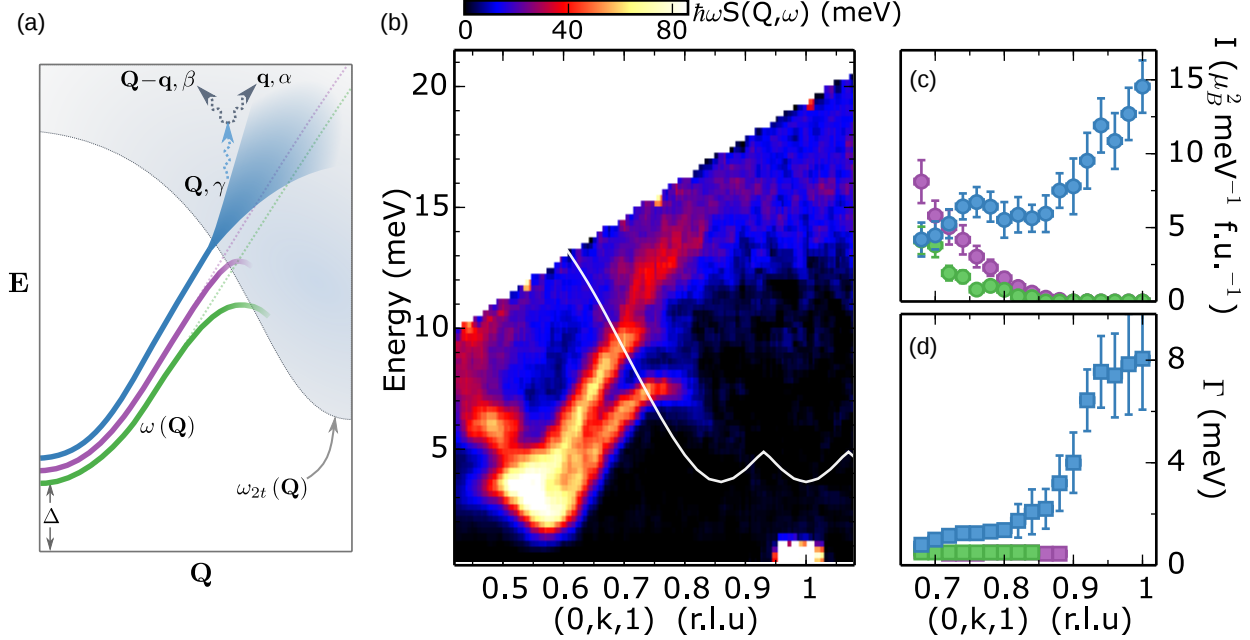


FIG. 4. Level repulsion and termination of quasiparticle spectrum in BiCu_2PO_6 . (a) Schematic illustration of the renormalization and termination of different single-triplon branches as they approach the multi-triplon continuum. Within the continuum a single triplon with momentum \mathbf{Q} and spin quantum number γ can decay into two triplons with momentum \mathbf{q} and $\mathbf{Q} - \mathbf{q}$. (b) $\hbar\omega S(\mathbf{Q}, \omega)$ highlighting the avoided crossing of the triplon branches with the continuum scattering around \mathbf{Q}_c . Solid white line is the lower bound for two-triplon scattering calculated from the non-interacting bond-operator theory. Momentum dependence of the spectral weight contained in each branch (c) and full width half maximum (d).

Supplementay Information: Quasiparticle-continuum level repulsion in a quantum magnet

Appendix A: Bond Operator Theory

Considering the valence bond crystal order with valence bonds at the J_4 links in BiCu_2PO_6 we have calculated triplon excitation spectrum within the framework of bond operator theory as described below. To describe spin dynamics in BiCu_2PO_6 we employ a general spin Hamiltonian with Heisenberg J_{ij} , Dzyaloshinskii-Moriya \mathbf{D}_{ij} , and anisotropic symmetric $\Gamma_{ij}^{\mu\nu}$ exchange interactions

$$\mathcal{H} = \sum_{i>j} (J_{ij} \mathbf{S}_i \cdot \mathbf{S}_j + \mathbf{D}_{ij} \cdot \mathbf{S}_i \times \mathbf{S}_j + \Gamma_{ij}^{\mu\nu} S_i^\mu S_j^\nu) - g\mu_B \mathbf{H} \cdot \sum_i \mathbf{S}_i, \quad (\text{A1})$$

where summations over $\mu, \nu (= x, y, z)$ are assumed. The symmetric anisotropy term is constrained by the relation

$$\Gamma_{ij}^{\mu\nu} = \frac{D_{ij}^\mu D_{ij}^\nu}{2J_{ij}} - \frac{\delta^{\mu\nu} \mathbf{D}_{ij}^2}{4J_{ij}}. \quad (\text{A2})$$

Hence, for a given link, J_{ij} and \mathbf{D}_{ij} are regarded as free parameters with $\Gamma_{ij}^{\mu\nu}$ determined by the former. The coupling constants in the Hamiltonian are constrained with the space group symmetry $Pnma$ into J_n , \mathbf{D}_n , and $\Gamma_n^{\mu\nu}$ ($n = 1, \dots, 4$) as introduced in main part of the paper. In our theory, the anisotropic interactions \mathbf{D}_3 , and $\Gamma_3^{\mu\nu}$ at J_3 links are ignored since J_3 is already significantly small compared to the other Heisenberg interactions.

Following standard procedures in bond operator theory [1–3], we rewrite the Hamiltonian by using the bond operator representations for the spins $\mathbf{S}_{L,R}$ in each dimer at J_4 links

$$S_{L,R}^\alpha = \pm \frac{1}{2} (s^\dagger t_\alpha + t_\alpha^\dagger s) - \frac{i}{2} \epsilon_{\alpha\beta\gamma} t_\beta^\dagger t_\gamma, \quad (\text{A3})$$

where $\alpha, \beta, \gamma \in \{x, y, z\}$ and $\epsilon_{\alpha\beta\gamma}$ is the totally antisymmetric tensor. Here, the bond operators s^\dagger and t_α^\dagger create the spin-singlet and spin-triplet states at the dimer respectively. We require the bosonic statistics for the bond operators. The bond operator representation enlarges the Hilbert space so that we restrict it to the physical Hilbert space by allowing only one bond particle at a dimer via the Lagrange multiplier μ : $-\mu(s^\dagger s + t_\alpha^\dagger t_\alpha - 1)$. On top of that, the s -bosons are condensed to describe the valence bond crystal phase: $\langle s \rangle = \langle s^\dagger \rangle = \bar{s}$.

After all above procedures, the bond operator Hamiltonian has the form $\mathcal{H} = \mathcal{H}_{\text{quad}} + \mathcal{H}_{\text{cubic}} + \mathcal{H}_{\text{quartic}}$, where $\mathcal{H}_{\text{quad}}$ consists of quadratic terms of t -boson operators, and so forth.

We consider the quadratic part \mathcal{H}_{quad} for the description of single-triplon excitations in BiCu_2PO_6 . The quadratic bond operator Hamiltonian is diagonalized through Bogoliubov transformation:

$$\mathcal{H}_{quad} = E_{gr} + \sum_{\mathbf{Q}} \sum_{n=1}^6 \omega_n(\mathbf{Q}) \gamma_n^\dagger(\mathbf{Q}) \gamma_n(\mathbf{Q}), \quad (\text{A4})$$

where $\gamma_n(\mathbf{Q})$ is the Bogoliubov quasiparticle, here triplon, operator with the excitation energy $\omega_n(\mathbf{Q})$. Here, \mathbf{Q} is momentum and n is band index of the triplon excitation spectrum. The ground state is determined by the equations $\partial E_{gr}/\partial \bar{s} = \partial E_{gr}/\partial \mu = 0$.

As already discussed in main body of the paper, neutron scattering measurement data is well reproduced in the bond operator theory with the following set of coupling constants: $J_1 = J_2 = J_4 = 8$ meV, $J_3 = 1.6$ meV, $D_1^a = 0.6J_1$, $D_1^b = 0.45J_1$, $\Gamma_1^{aa} = 0.039J_1$, $\Gamma_1^{bb} = -0.039J_1$, and $\Gamma_1^{ab} = \Gamma_1^{ba} = 0.135J_1$. With this set of coupling constants, the ground state has $\bar{s} = 0.869$, $\mu = -1.693J_1$. Comparing with the case of an isolated dimer ($\bar{s} = 1$, $\mu = -0.75J$), we notice that the valence bonds in BiCu_2PO_6 are quite soft with significant fluctuations, which is attributed to strong inter-dimer interactions ($J_{1,2,3}$, D_1 , Γ_1) comparable to intra-dimer interaction (J_4). An important comment is followed. In the quadratic Hamiltonian \mathcal{H}_{quad} , the DM terms with the coupling constant \mathbf{D}_1 cancel and do not explicitly enter the Hamiltonian, rather it is the symmetric anisotropic interaction which is essential for describing magnetic anisotropy in BiCu_2PO_6 . Of course the existence of a large symmetric anisotropy term necessarily implies a large antisymmetric DM term through Eq. A2.

The bond operator theory approach was able to successfully capture the magnetic field dependence of triplon excitations for $H \parallel \mathbf{a}$ as measured by neutron scattering. However, as an additional test of the theory we may explore predictions for the Zeeman behaviour of the triplon bands with magnetic fields applied along the other axes of the crystal. This can provide information about the anisotropic critical fields which have been measured by high field magnetization experiments [4]. The Zeeman energy of the triplon bands at the dispersion minimum $\mathbf{Q} = (0, 0.575, 1)$ calculated within the bond operator theory are plotted in Fig. S1. Each band has a characteristic field direction, where the Zeeman dependence is flat, with negligible field dependence. The critical magnetic field H_c at which the spin gap is closed can be obtained by extrapolating the data points for each applied magnetic field direction, giving $H_c^a \approx 25$ T, $H_c^b \approx 21$ T, and $H_c^c \approx 19$ T roughly in agreement with measured critical fields [4]. Besides the hierarchy in the critical fields, a rather curious

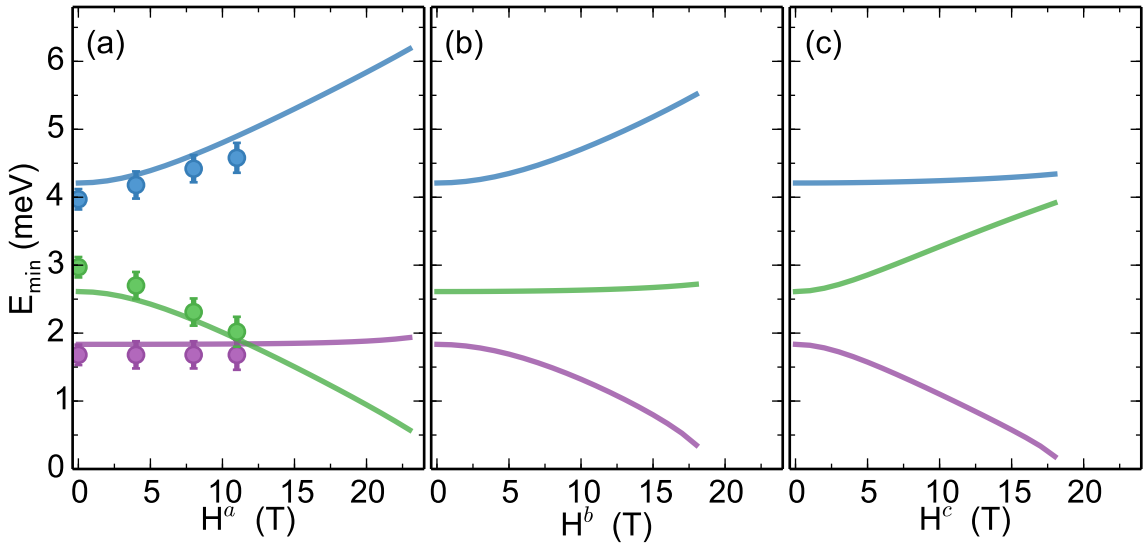


FIG. S1. Calculated Zeeman energy of each mode at $Q = (0, 0.575, 1)$ from the bond operator theory. In (a) the neutron scattering data for applied fields up to 11 T is included.

Zeeman behavior is revealed in Fig. S1 which shows the magnetic field dependent energy of each band is strongly coupled to the applied field direction with the modes having the relative Zeeman character of $S_z = \{0, +1, -1\}$, $\{+1, 0, -1\}$, and $\{+1, -1, 0\}$ for fields applied along the **a**, **b**, and **c** axis respectively. Here, S_z means the spin component along the field direction.

[1] S. Sachdev and R. N. Bhatt, Phys. Rev. B **41**, 9323 (1990).
[2] S. Gopalan, T. M. Rice, and M. Sigrist, Phys. Rev. B **49**, 8901 (1994).
[3] M. Matsumoto, B. Normand, T. M. Rice, and M. Sigrist, Phys. Rev. B **69**, 054423 (2004).
[4] Y. Kohama, S. Wang, A. Uchida, K. Prsa, S. Zvyagin, Y. Skourski, R. D. McDonald, L. Balicas, H. M. Rønnow, C. Rüegg, and M. Jaime, Phys. Rev. Lett. **109**, 167204 (2012).